Multifunctional electrospun CS/PVA/AgNPs nanofiber membranes for dye removal and antimicrobial water purification

Nguyen Thi Anh Huy, Tran Thanh Viet, Nguyen Khoi Nguyen, Le Anh Kien*

Institute for Tropical Technology, Academy of Military Science and Technology, 57A Truong Quoc Dung, Phu Nhuan, Ho Chi Minh City, Vietnam.
*Corresponding author: leanhkien@vittep.com
Received 23 Sep. 2025; Revised 18 Nov. 2025; Accepted 31 Dec. 2025; Published 25 Feb. 2026.
DOI: https://doi.org/10.54939/1859-1043.j.mst.109.2026.113-120

ABSTRACT

There is an urgent need for sustainable methods to purify water contaminated with dyes and pathogenic microorganisms. Conventional treatment technologies often face limitations due to the use of toxic chemicals or complex fabrication processes. In this study, electrospun chitosan/poly(vinyl alcohol)/silver nanoparticle (CS/PVA/AgNPs) nanofiber membranes were fabricated and evaluated for their dual functionality in dye removal and antibacterial activity. SEM, XRD, and EDS analyses confirmed the formation of quasi-spherical AgNPs and their uniform distribution within the polymer matrix. Morphological analysis revealed that the incorporation of AgNPs into the CS/PVA matrix reduced the fiber diameter from 120-230 nm to 99-158 nm and significantly decreased bead formation. Congo Red adsorption reached equilibrium within 120-150 min, with capacities increasing with dye concentration. Maximum adsorption occurred at pH 4, and the membrane retained over 60% efficiency after two regeneration cycles. Additionally, the CS/PVA/AgNPs membrane exhibited strong antibacterial activity, achieving up to 99% inhibition against Escherichia coli and Staphylococcus aureus. Overall, these results highlight the potential of CS/PVA/AgNPs nanofiber membranes as multifunctional, eco-friendly materials for simultaneous dye adsorption and antimicrobial water purification.

Keywords: Electrospinning; Dye removal; Antibacterial activity; Water treatment.

1. INTRODUCTION

Water pollution remains a critical challenge, largely driven by industrial effluents containing synthetic dyes and pathogens, which threaten ecosystems and human health. Around 700,000 tons of dyes, many toxic or carcinogenic, enter water bodies annually, while viral contamination affects about 2 billion people [1]. Conventional treatments, including coagulation, biological processes, and activated charcoal, have limitations in removing complex dyes or ensuring reusability, and chemical disinfectants may produce harmful byproducts. The limitations presented by each method listed outline the need for a different approach that is innovative, cost-effective, and sustainable.

Advanced membrane technologies, especially electrospun nanofiber membranes, have gained attention as efficient and eco-friendly solutions for water purification. Their nanoscale fibers provide high surface area and small pore sizes suitable for diverse applications. Blending biopolymers enables synergistic properties, with chitosan/polyvinyl alcohol (CS/PVA) nanofibers emerging as an excellent candidate for water remediation due to their adjustable porosity and multifunctionality. Chitosan (CS), a biodegradable polymer derived from chitin, demonstrates outstanding dye adsorption capacity due to the presence of amino and hydroxyl groups that facilitate strong electrostatic interactions with anionic dye molecules. It is also well recognized for its antibacterial properties and widely used as a biomaterial. However, when used alone, CS readily loses mechanical strength due to its variation in deacetylation degrees and molecular weights, thereby shortening its degradation time. Previous studies have demonstrated that the tensile strength increased markedly as the PVA mass ratio rose in the PVA/CS matrix [2, 3]. This enhancement is attributed to intermolecular interactions between CS and PVA, primarily hydrogen

bonding between the hydroxyl groups of PVA and the -NH_2 or -OH groups of CS [4]. As the PVA content increased, these interactions became stronger, resulting in improved tensile strength of the crosslinked PVA/CS nanofibrous mats. Combining with PVA, a hydrophilic polymer that has high mechanical properties, has led the resulting nanofibers to gain improved stability and mechanical strength [2, 5], making them suitable for diverse filtration applications.

To improve membrane functionality, especially antibacterial performance, metallic nanoparticles – particularly silver nanoparticles (AgNPs) – are commonly incorporated. These AgNPs possess remarkable antibacterial and antifungal activity, effectively neutralizing pathogens such as *Escherichia coli (E. coli)*, *Staphylococcus aureus (S. aureus)*, and *Candida albicans* due to their small size and large surface area, which facilitate effective interaction with microbial cells. Owing to these properties, AgNPs are widely used as potent antimicrobial agents.

This study developed and characterized electrospun CS/PVA/AgNPs nanofiber films, evaluating their Congo Red adsorption under varying conditions and fitting kinetic-isotherm models to understand the mechanism. Eventually, the antibacterial ability of CS/PVA/AgNPs membranes regarding *E. coli* and *S. aureus* was evaluated, demonstrating promising potential for advanced water treatment.

2. EXPERIMENTAL

2.1. Materials

Fresh betel leaves are collected from Hoc Mon Province, Viet Nam. Chitosan (viscosity ≤ 150 cPs) was obtained from Vietnam Food Joint Stock Company. Polyvinyl alcohol (PVA, ≥ 99%), acetic acid (CH_3COOH, ≥ 99.5%), ethanol (C_2H_5OH, 99.5%), and silver nitrate ($AgNO_3$, > 99.8%) were purchased from commercial suppliers and used without further purification. All solutions were prepared using distilled water.

2.2. Fabrication of the silver nanoparticle solution

The *Piper betle* (L.) leaf extract was obtained by dispersing dried leaf powder in 80% ethanol and stirring at 50 °C for 45 min. The extraction was repeated three times, and combined filtrates were vacuum-evaporated at 45 °C for 45 min. A portion of this extract was redissolved in 80% ethanol and added dropwise to a 10 mM silver nitrate solution, followed by stirring at 50 °C for 5 h to synthesize silver nanoparticles.

2.3. Fabrication of the CS/PVA/AgNPs solution

A 2 wt.% CS solution was prepared by dissolving CS in 2 wt.% acetic acid at 50 °C for 1 h, while a 5 wt.% PVA solution was obtained by dissolving PVA in water at 70 °C for 1 h. The two solutions were then mixed at a CS/PVA mass ratio of 3:6 and stirred for 15 min. Subsequently, the AgNPs solution was added to the mixture and further stirred at room temperature for 15 min, resulting in a CS/PVA/AgNPs formulation with a mass ratio of 3:6:1 for further processing.

2.4. Electrospinning process

The prepared mixture solution was loaded into a syringe of the electrospinning apparatus. The process parameters were set as follows: drum speed of 300 rpm, applied voltage of 20 kV, a collecting distance of 13 cm, and a flow rate of 1 mL/h. Electrospinning was subsequently carried out to produce the CS/PVA/AgNPs nanofiber membrane.

2.5. Characterization of electrospun CS/PVA/AgNPs nanofiber membrane

The morphology of the electrospun CS/PVA/AgNPs nanofibers was examined using scanning electron microscopy (SEM, TESCAN MIRA) operated at an acceleration voltage of 5 keV. To further probe the molecular interactions among CS, PVA, and AgNPs, Fourier transform infrared spectroscopy (FTIR, Bruker Alpha II) was performed in transmittance mode over the spectral range of 4000 - 500 cm^{-1}.

2.6. Adsorption experiment

The adsorption experiments were performed at various initial CR concentrations (25 - 200 mg/L), contact times (5 - 150 min), pH (2 - 10) and regeneration cycles with a fixed adsorbent dosage of 1:1000 (g/mL) applied in all experiments. Each sample was placed in a dye solution and performed at room temperature for certain times. For the regeneration experiments, a constant contact time of 1 h was applied. Residual dye concentrations were measured using UV-Vis spectroscopy at 497 nm.

2.7. Experimenting with antibacterial activity

The antibacterial activity of CS/PVA/AgNPs nanofiber membranes against *E. coli* and *S. aureus* was evaluated using an OD600 growth inhibition assay. Sterilized membranes (2 × 2 cm) were incubated with bacterial suspensions in LB broth at 37 °C for 24 h, and bacterial growth was quantified by measuring OD600.

3. RESULTS AND DISCUSSION

3.1. Morphology of electrospun CS/PVA/AgNPs nanofiber membrane

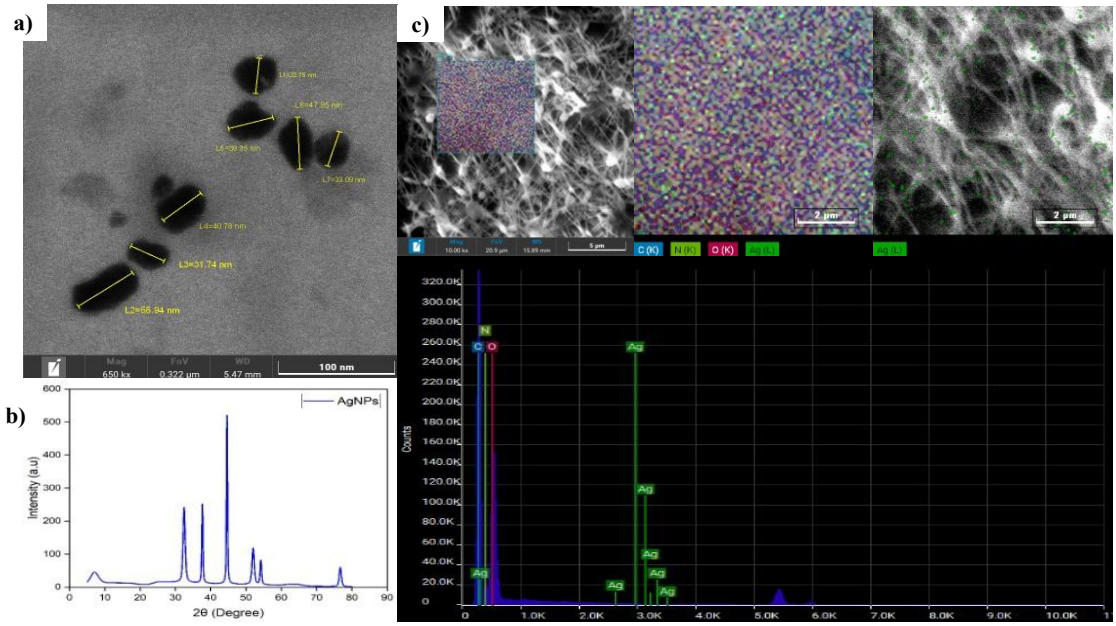

Figure 1. *SEM image of the synthesized AgNPs (a), XRD analysis of AgNPs synthesized from betel leaf extract (b) and EDS analysis of the CS/PVA/AgNPs membrane (c).*

Figure 1a displays AgNPs biosynthesized using betel leaf extract, exhibiting quasi-spherical shapes with diameters ranging from 32 to 56 nm and an average size of approximately 40 nm. Although there are small clusters formed due to the agglomeration, their boundaries remain distinguishable, allowing a clear assessment of their overall shape and distribution. In addition, their surfaces are relatively smooth, which contributes to enhancing their efficiency of contact between the particles and bacterial cells. XRD analysis (figure 1b) confirms high crystallinity, with diffraction peaks at 37.66°, 44.61°, and 76.71° corresponding to the (111), (200), and (311) planes of face-centered cubic silver (JCPDS 04-0783). However, the peak at around 64° is replaced by a broad band between 62° and 64°, which may be caused by the presence of many organic compounds in the betel leaf extract surrounding the AgNPs, creating a background noise that weakens this peak. Similarly, the appearance of background interference in the XRD pattern may also result from the presence of these complex biological molecules. The elemental mapping results further confirm the presence and distribution of AgNPs within the CS/PVA matrix (figure

1c). The Ag-mapping image shows numerous green-highlighted spots uniformly dispersed throughout the polymer network. This homogeneous distribution indicates that the AgNPs were effectively stabilized by the CS/PVA matrix, preventing aggregation – a common issue in metallic nanoparticle-based systems. Such uniform dispersion is crucial for ensuring consistent antimicrobial performance of the membrane.

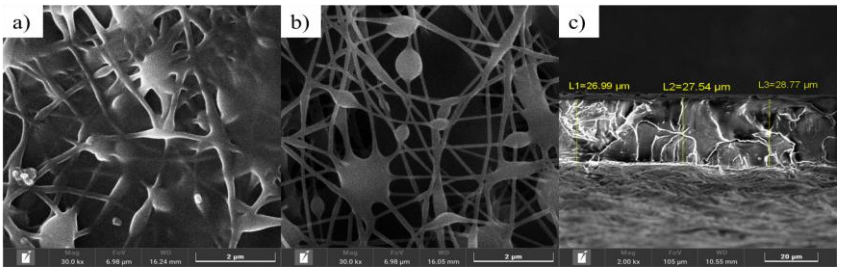

Figure 2. *SEM images of (a) CS/PVA, (b) CS/PVA/AgNPs membrane and (c) the crossing surface of the CS/PVA/AgNPs membrane.*

The pure CS/PVA membrane exhibits fiber diameters of 120-230 nm with noticeable bead formation (figure 2a). After incorporating AgNPs (figure 2b), the fiber diameters decrease to 99-158 nm and bead formation is reduced. These changes result from viscosity and charge variations in the CS/PVA/AgNPs solution: the AgNPs solution lowers the initially high viscosity of CS, while the charge of AgNPs slightly increases the charge density of the solution, enhancing jet stretching during electrospinning and producing finer fibers [6]. A cross-sectional image of the CS/PVA/AgNPs membrane is shown in figure 2c. The membrane fabricated from electrospun nanofibers appears fully densified, with no visible pores. The average thickness of the membrane after electrospinning was measured to be 27.77 ± 0.91 µm. Controlling the value of thickness is necessary for water treatment applications, when permeability and water flux are important factors.

3.2. Chemical composition

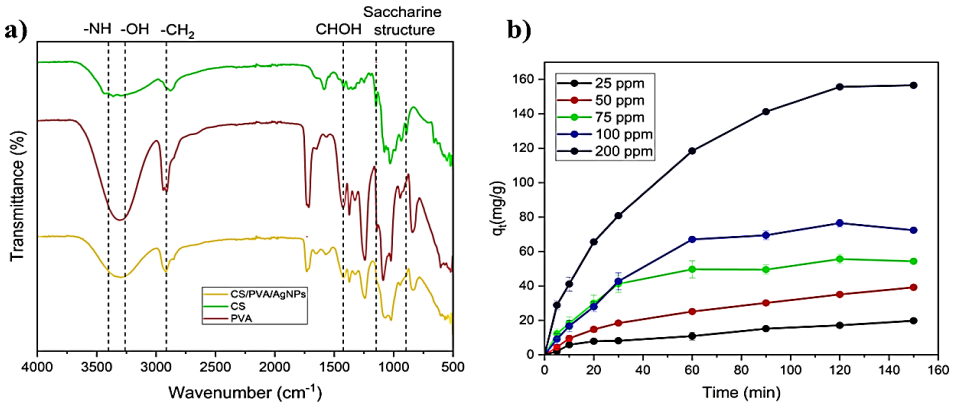

Figure 3. *FTIR spectra of the CS/PVA/AgNPs membrane (a) and adsorption capacity of CS/PVA/AgNPs membrane by time at different initial concentrations (b).*

The chemical structure of the electrospun CS/PVA/AgNPs nanofiber membrane was analyzed using FTIR spectroscopy (figure 3a). A broad band at 3000 - 3500 cm^{-1} corresponds to O-H stretching in PVA as well as $-NH_2$ and -OH groups in CS, with its reduced intensity in the CS/PVA/AgNPs membrane indicating interactions between the two polymers [7]. The peak at 2914 cm^{-1} represents $-CH_2$ stretching, while the band at 1424 cm^{-1} is assigned to CH-O-H bending [7]. An additional band in the 800-1200 cm^{-1} region reflects the saccharide structure of chitosan [8]. These findings confirm the presence of characteristic functional groups in the CS/PVA/AgNPs membrane, consistent with those identified in the individual CS and PVA spectra.

3.3. Adsorption studies

As shown in figure 3b, the adsorption capacity increased markedly during the first 120 minutes, after which it reached equilibrium and then gradually declined at initial concentrations of 75 and 100 ppm. In contrast, at 25 and 50 ppm, the adsorption capacity exhibited a slight increase after 120 minutes. The slight decrease in adsorption at initial concentrations of 75 and 100 ppm may be associated with partial desorption of weakly bound CR molecules, which detach from the surface as the system approaches equilibrium. At high dye concentrations, strong intermolecular competition and repulsive interactions among adsorbed CR molecules can also cause some previously adsorbed molecules to be displaced back into the solution. After 150 min, adsorption capacities were 19.84, 39.19, 54.38, 72.37, and 156.57 mg/g for increasing dye concentrations. Higher concentrations enhance diffusion into the nanofiber pores, increasing contact with available adsorption sites.

Table 1. *Isotherm fitting parameters of CS/PVA/AgNPs for CR adsorption.*

Langmuir model			**Freundlich model**		
k_L (L/mg)	**q_{max} (mg/g)**	**R^2**	**k_f (L/mg)**	**1/n**	**R^2**
1015.3333	3333.3333	0.3467	3.4991	0.9695	0.9994

To clarify the adsorption mechanism, the isotherm data were fitted to the Freundlich and Langmuir models (table 1). Among the two models, the Freundlich isotherm exhibited the best fit, with the highest correlation coefficient (R^2 = 0.9994). This indicates that the Freundlich equation most accurately describes the adsorption equilibrium of the dye on the CS/PVA/AgNPs nanofiber membrane. The value of n = 1.0315, which lies within the range of 1-10, indicates that the adsorption process is favorable [9]. Moreover, this model suggests that multilayer adsorption occurs on the electrospun membrane surface.

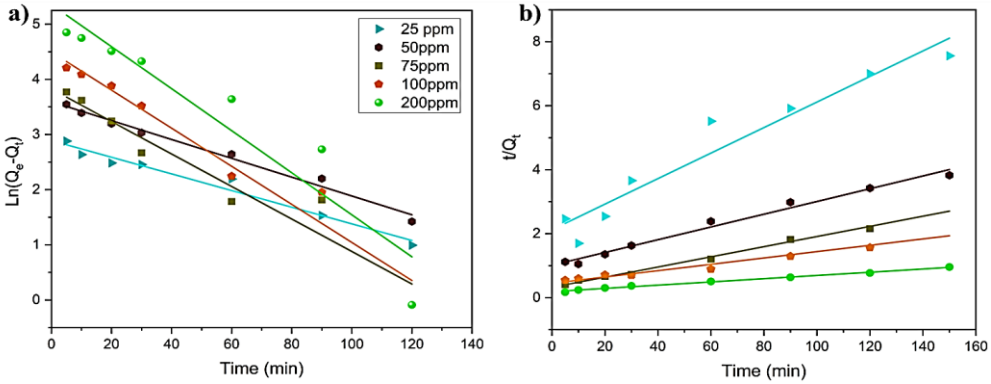

Figure 4. *The pseudo-first-order (a) and pseudo-second-order (b) adsorption models of CR by the CS/PVA/AgNPs nanofiber membrane.*

Figure 4 shows the linear fittings of the pseudo-first-order and pseudo-second-order kinetic models, with table 2 summarizing the corresponding parameters. As shown in the table, the correlation coefficients (R^2) obtained from the pseudo-first-order kinetic model – 0.971 and 0.9857 for the concentrations of 25 and 50 ppm, respectively – are higher than those from the pseudo-second-order kinetic model. Otherwise, the R^2 for the concentrations of 75, 100, and 200 ppm are higher than that from pseudo-first order. At the lower concentrations, the adsorption process depends mainly on the available sites on the surface of the material; thus, the dye molecules' interaction with the membrane was controlled by physical adsorption. However, when increasing the concentration gradually, the number of vacant sites for dye molecules is reduced as well. The adsorption process now depends on the sharing and exchanging of electrons between the adsorbents and adsorbates, which can be considered the rate-controlling step [10].

Table 2. *Kinetic parameters of CR adsorption on CS/PVA/AgNPs membrane.*

Initial concentration	Pseudo-first order			Pseudo-second order		
	$Q_{e,cal}$ (mg/g)	K_1 (1/min)	R^2	$Q_{e,cal}$ (mg/g)	K_2 (g/mg.min)	R^2
25	17.9843	0.0151	0.9713	25.0627	7.4943×10^{-4}	0.9345
50	36.3575	0.0171	0.9857	50.2513	3.9035×10^{-4}	0.9852
75	40.9233	0.0250	0.8820	64.9351	7.0062×10^{-4}	0.9923
100	78.1086	0.0290	0.9594	114.9425	1.5545×10^{-4}	0.9763
200	211.5159	0.0381	0.8974	198.0198	1.3446×10^{-4}	0.9927

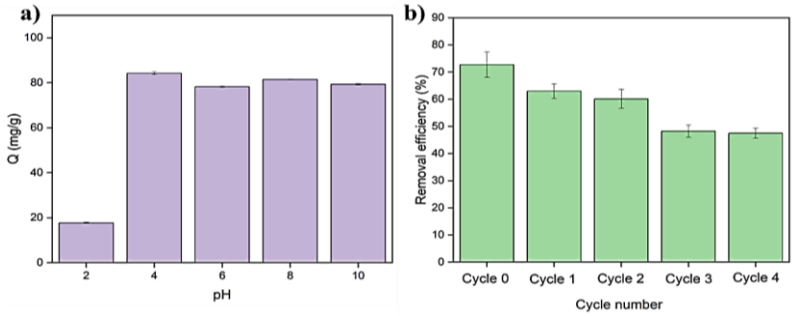

Figure 5*. Effect of pH (a) and number of reuse cycles (b) on dye adsorption by the CS/PVA/AgNPs membrane.*

As shown in figure 5a, dye removal was significantly slower under acidic conditions, especially when the solution pH was below 4 (17.47 mg/g). The highly acidic environment causes partial dissolution and disruption of the membrane structure, which further reduces porosity and destroys some active binding sites. These combined effects significantly limit adsorption despite favorable charge interactions. The highest adsorption capacity – 84.19 mg/g for an initial CR concentration of 100 mg/L – was achieved at pH 4.0. This improvement suggests that partial deprotonation of chitosan functional groups resulted in increasing the availability of adsorption sites. When the pH exceeded 4.0, the removal efficiency remained nearly constant up to pH 10.0. The stability of adsorption efficiency across this wide pH range reflects the structural robustness imparted by the polymer matrix.

3.4. Reusability performance of the adsorbent

The regeneration performance, an important indicator of adsorption efficiency, was also examined, and the results are presented in figure 5b. As shown, the removal efficiency decreased gradually with increasing cycle number. The efficiency declined to 63% and 60% in Cycle 1 and Cycle 2, respectively, suggesting partial loss of active sites after repeated use. The decline in Cycle 3 and Cycle 4 suggests that prolonged immersion and repeated regeneration may weaken the membrane network or cause partial leaching of loosely bound components. Overall, the results demonstrate that the adsorbent possesses moderate reusability, maintaining more than 60% of its initial performance after two regeneration cycles. Further incorporation of additional reinforcing components or improved crosslinking density to enhance long-term durability in aqueous systems may be necessary to enhance the cycle durability of the material.

3.5. Evaluation of antimicrobial activity

Figure 6 shows the growth inhibition by CS/PVA/AgNPs membranes, measured via optical density at 600 nm for *E. coli* and *S. aureus*. Owing to their strong antibacterial properties, metals are widely employed in the treatment of various bacteria, especially AgNPs. Previous studies have demonstrated that AgNPs exhibit strong antibacterial activity owing to their isotropic geometries, such as spherical shapes, which provide a large surface-to-volume ratio [11]. Because of their strong antibacterial activity, these silver nanoparticles have been widely used in water treatment.

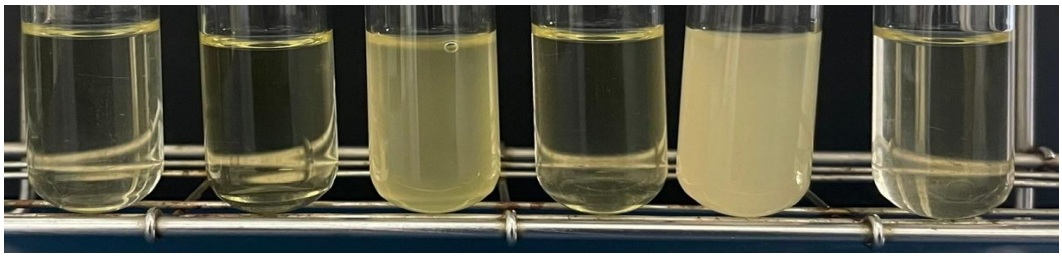

(a) (b) (c) (d) (e) (f)

Figure 6. *Antibacterial activity of CS/PVA/AgNPs membrane: (a) LB broth; (b) CS/PVA/AgNPs control; (c) E. coli control; (d) CS/PVA/AgNPs E. coli; (e) S. aureus control; (f) CS/PVA/AgNPs S. aureus.*

Table 3. *Growth inhibition of AgNPs and CS/PVA/AgNPs membranes.*

Material	**Bacteria growth inhibition (%)**	
	Escherichia coli	*Staphylococcus aureus*
AgNPs	98.44	99.35
CS/PVA/AgNPs	99.00	99.84

As shown in table 3, incorporating AgNPs into the CS/PVA matrix significantly enhanced the antibacterial performance compared to single AgNPs. Although chitosan inherently exhibits antibacterial activity, its efficiency against *E. coli* and *S. aureus* is relatively low. However, the presence of chitosan in the membrane still plays an important supporting role because its protonated amino groups ($-NH_3^+$) can interact electrostatically with negatively charged bacterial cell membranes [12], increasing membrane permeability and making bacteria more susceptible to silver-induced damage. This synergistic effect facilitates closer contact between AgNPs and bacterial cells, thereby improving overall antibacterial efficiency. The obtained membrane presents the inhibition toward these two bacteria at almost 100% and can be compared to other materials such as polycaprolactone/polyethylene oxide/chitosan/cetyl trimethyl ammonium bromide [13], conjugated microporous polymers/AgNPs [14], and silver-based metal-organic frameworks [15]. These results show that introducing silver nanoparticles in CS/PVA nanofibers using electrospinning is an effective way to develop a material for bacterial removal.

4. CONCLUSIONS

In this study, CS and PVA were used to fabricate electrospun nanofiber membranes incorporated with AgNPs for water treatment applications. Morphological analysis revealed that CS/PVA/AgNPs nanofiber membranes were successfully fabricated with finer, more uniform fibers and well-dispersed AgNPs. The membrane showed strong adsorption of CR, reaching equilibrium within 120-150 min, following the Freundlich isotherm and exhibiting a shift from pseudo-first-order to pseudo-second-order kinetics with increasing dye concentration. Maximum adsorption occurred at pH 4, and the membrane retained over 60% efficiency after two regeneration cycles. Additionally, it achieved up to 99% antibacterial inhibition against *E. coli* and *S. aureus*. Overall, these findings suggest that the electrospun CS/PVA/AgNPs nanofiber membrane is a promising material for the simultaneous removal of CR dye and bacteria from contaminated water.

Acknowledgement: *The authors gratefully acknowledge the support of Academy of Military Science and Technology and Institute for Tropical Technology through funding provided under grant number ĐTVCBT.20-3/VNĐMT.*

REFERENCES

[1]. World Health Organization, *"Guidelines for drinking-water quality"*, 3rd ed., vol. 1. Geneva, Switzerland: WHO Press, (2004).

[2]. E. Abdelrazek et al., *"The accessibility of change of the structural, morphological and thermal properties by intermolecular hydrogen bonding in PEO/PVA blend containing $MnCl_2$"*, International Journal of Modern Applied Physics, vol. 1, no. 1, pp. 83–96, (2012).
[3]. M. Koosha et al., *"Electrospinning, mechanical properties, and cell behavior study of chitosan/PVA nanofibers"*, Journal of Biomedical Materials Research Part A, vol. 103, no. 9, pp. 3081–3093, (2015).
[4]. H. Zheng et al., *"Preparation and characterization of chitosan/poly(vinyl alcohol) blend fibers"*, Journal of Applied Polymer Science, vol. 80, no. 13, pp. 2558–2565, (2001).
[5]. Elashmawi et al., *"Modification and development of electrical and magnetic properties of PVA/PEO incorporated with $MnCl_2$"*, Physica B: Condensed Matter, vol. 434, pp. 57–63, (2014).
[6]. K. Selvam et al., *"Polyacrylonitrile/silver nanoparticle electrospun nanocomposite matrix for bacterial filtration"*, Fibers and Polymers, vol. 16, no. 6, pp. 1327–1335, (2015).
[7]. G. Açık et al., *"Effect of polyvinyl alcohol/chitosan blend ratios on morphological, optical, and thermal properties of electrospun nanofibers"*, Turkish Journal of Chemistry, vol. 43, no. 1, pp. 137–149, (2019).
[8]. C. Branca et al., *"Role of the OH and NH vibrational groups in polysaccharide-nanocomposite interactions: A FTIR-ATR study on chitosan and chitosan/clay films"*, Polymer, vol. 99, pp. 614–622, (2016).
[9]. G. Crini et al., *"Removal of CI Basic Green 4 (Malachite Green) from aqueous solutions by adsorption using cyclodextrin-based adsorbent: Kinetic and equilibrium studies"*, Separation and Purification Technology, vol. 53, no. 1, pp. 97–110, (2007).
[10]. Z. Wang et al., *"Highly regenerable alkali-resistant magnetic nanoparticles inspired by mussels for rapid selective dye removal offer high-efficiency environmental remediation"*, Journal of Materials Chemistry A, vol. 3, no. 39, pp. 19960–19968, (2015).
[11]. Albanese et al., *"The effect of nanoparticle size, shape, and surface chemistry on biological systems"*, Annual Review of Biomedical Engineering, vol. 14, no. 1, pp. 1–16, (2012).
[12]. P. Sahariah et al., *"Antimicrobial chitosan and chitosan derivatives: A review of the structure–activity relationship"*, Biomacromolecules, vol. 18, no. 11, pp. 3846–3868, (2017).
[13]. L. Li et al., *"Preparation and antibacterial properties of a composite fiber membrane material loaded with cationic antibacterial agent by electrospinning"*, Nanomaterials, vol. 13, no. 3, p. 583, (2023).
[14]. H. Sun et al., *"Tissue paper-like conjugated microporous polymers film for bacteria inhibition"*, Journal of Environmental Chemical Engineering, vol. 10, no. 6, p. 108933, (2022).
[15]. Arenas-Vivo et al., *"Antiadherent AgBDC metal–organic framework coating for Escherichia coli biofilm inhibition"*, Pharmaceutics, vol. 15, no. 1, p. 301, (2023).

TÓM TẮT

Màng sợi nano CS/PVA/AgNPs đa chức năng được chế tạo bằng phương pháp kéo sợi điện trường để loại bỏ thuốc nhuộm và khử khuẩn trong xử lý nước

Hiện nay, có một nhu cầu cấp thiết về các phương pháp bền vững để làm sạch nước bị ô nhiễm bởi thuốc nhuộm và vi sinh vật gây bệnh. Các công nghệ xử lý nước truyền thống thường gặp hạn chế do sử dụng hóa chất độc hại hoặc quy trình chế tạo phức tạp. Trong nghiên cứu này, màng sợi nano chitosan/poly(vinyl alcohol)/nano bạc (CS/PVA/AgNPs) được chế tạo bằng phương pháp kéo sợi điện trường và được đánh giá về khả năng kép trong việc loại bỏ thuốc nhuộm và kháng khuẩn. Các kết quả SEM, XRD và EDS xác nhận sự hình thành các hạt AgNPs có dạng gần giống hình cầu và phân bố đồng đều trong ma trận polymer. Phân tích hình thái màng cho thấy việc kết hợp AgNPs vào ma trận CS/PVA giúp làm giảm đường kính sợi từ 120-230 nm xuống 99-158 nm, đồng thời hạn chế đáng kể sự hình thành hạt. Quá trình hấp phụ Congo Red đạt trạng thái cân bằng trong 120-150 phút, với dung lượng hấp phụ tăng theo nồng độ của thuốc nhuộm. Khả năng hấp phụ tối đa đạt được ở pH 4, và màng duy trì hiệu suất loại bỏ trên 60% sau hai chu kỳ tái sử dụng. Ngoài ra, màng CS/PVA/AgNPs còn thể hiện hoạt tính kháng khuẩn mạnh, ức chế tới 99% đối với Escherichia coli và Staphylococcus aureus. Nhìn chung, các kết quả này cho thấy màng nano sợi CS/PVA/AgNPs là vật liệu đa chức năng, thân thiện với môi trường, có tiềm năng ứng dụng trong việc loại bỏ thuốc nhuộm và khử khuẩn nước đồng thời.

Từ khoá: Kéo sợi điện trường; Loại bỏ thuốc nhuộm; Hoạt tính kháng khuẩn; Xử lý nước.